

Effect of Linear Elongation of PDMS-Supported Polyelectrolyte Multilayer Determined by Attenuated Total Reflectance IR Radiation

Johannes Frueh,^{*,†} Gerald Reiter,[‡] Janos Keller,[‡] Helmuth Möhwald,[‡] Qiang He,^{*,†} and Rumen Krastev^{‡,§}

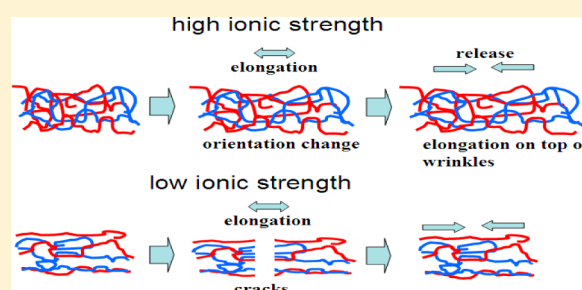
[†]Key Laboratory of Microsystems and Microstructures Manufacturing, Ministry of Education, Micro/Nano Technology Research Centre, Harbin Institute of Technology, Yikuang Street 2, Harbin 150080, China

[‡]Max Planck Institute of Colloids and Interfaces, Am Mühlenberg 1, 14424 Golm-Potsdam, Germany

[§]NMI Natural and Medical Sciences Institute at the University of Tübingen, Markwiesenstrasse 55, 72770 Reutlingen, Germany

S Supporting Information

ABSTRACT: Polyelectrolyte multilayers (PEMs) deposited on flexible supports, such as silicone rubber, show interesting properties upon elongation and release, like controlled wrinkling, elongation-based wetting, or dewetting and stimuli responsive nanovalves. To understand the underlying physical effects of PEM experiencing linear elongation, the orientation change of molecular groups within PEM experiencing linear elongation was investigated. The model PEM consists of polystyrenesulphonate and polydimethyldialyl chloride. The investigation method was infrared attenuated total reflectance. In the study, the orientation change of the benzene and the sulfate groups of polystyrenesulphonate upon elongation of the PEM, prepared at high and low ionic strengths, was tracked. The gained results show that the benzene group shows no sign of orientation change upon elongation, whereas the sulfate group does, whereby the reorientation depends on the ionic strength of the preparation solution. Upon release of elongation, the PEM prepared at low ionic strength shows no orientation change, whereas PEM prepared at high ionic strength does show further orientation change, indicating that the formed wrinkles elongate the PEM on the top of the wrinkles.



INTRODUCTION

LbL self-assembly of polyelectrolytes (PEs) is based on sequential adsorption of oppositely charged PEs.¹ The result is a polyelectrolyte multilayer (PEM) whose thickness, optical, electrical, and mechanical properties can be controlled with high precision.^{2–5} In many fields of application, the elongation-based properties of PEMs play an important role, like in the case of controlled wettability, controlled wrinkling, stimuli responsive nanovalves, or tissue engineering.^{3,6,7} To understand the underlying phenomena of these applications, the effect of elongation on the molecular structure has to be classified. Since the study of these properties requires PEM on flexible support materials, we used PEM supported by silicone rubber sheets (PDMS).^{3,7–9}

In an earlier study, the change in orientation of PE in elongated PEMs using pyrene-labeled PE was monitored by us.¹⁰ Since pyrene labels can theoretically affect the charge density of PE,¹¹ infrared attenuated total reflectance (IR-ATR) was the method of choice to investigate the orientation change of nonlabeled PE groups upon elongation of the PDMS-PEM system. IR-ATR is a well-known technique for infrared spectroscopy of thin films.^{12,13} One of the major requirements of this method is that the investigated substance needs to be deposited directly onto the ATR-crystal or at least in close

contact to the crystal.^{12,13} Simply placing polymer films in close contact to germanium crystals for quantitative results is not new, since Flournoy published results proving this principle in the year 1964.¹⁴ However, the published quantitative results using his approach are, according to the authors' knowledge, very scarce. Therefore, we explain the approach in the Materials section.

The samples were exposed to a unidirectional mechanical elongation of up to 15%. The ionic strength of the PEM preparation solution influences the molecular rearrangement upon elongation. A reorganization of molecules occurs in PEMs prepared at high ionic strength, but not in PEMs prepared at low ionic strength. Additionally, the sulfate and benzene groups of the PSS within the PEM react differently upon elongation. The benzene group showed, for both salt concentrations, no sign of reorientation, whereas the sulfate group changed the orientation in the case of high ionic strength. Upon release of elongation, the change in molecular orientation is not reversed. Additionally, an influence of the ionic strength on the PEM total signal intensity upon release is observed. This effect is

Received: October 30, 2012

Revised: February 5, 2013

Published: February 18, 2013

attributed to the fact that the preparation condition influences the resulting wrinkling structure³ of the PEM/PDMS system upon release of elongation.

MATERIALS AND METHODS

Materials. The PEM films were prepared from polystyrenesulphonate (PSS) (molecular weight (MW) = 70 000) and polydimethyldiallyl chloride (PDMA MW = 200 000–300 000, 20 wt % solution), and polyethylenimine (PEI MW = 750 000, 50 wt % solution, Sigma Aldrich, Germany). The ionic strength in the preparation solution was adjusted with NaCl (Merck KGaA, Darmstadt, Germany). All chemicals were used without further purification. The reason for choosing PDMA and PSS was that they are “strong” PEs, allowing a precise adjustment of the charge shielding and, therefore, the molecular confinement with the ionic strength.² Chem Draw images of PSS and PDMA can be seen in the Supporting Information, Figure S1. A laboratory water purification system from Elga Labwater, Germany, was used to obtain ultrapure water. The specific resistance of the water was higher than 18.2 MΩ·cm, the pH was 5.5, and the total organic carbon (TOC) content was less than 10 ppb.

PDMS slides were prepared by mixing Sylgard 184 (Dow Corning, Midland, MI) base and its curing agent in a 10:1 ratio. The mixture was cast into a plastic form and then cured for 12 h at 60 °C. Alternatively to PDMS from Dow Corning, a 10:1 mixture of polydimethylsiloxane, (vinyl-dimethyl terminated of 1000 centistokes viscosity) and 30–35% methylhydro-65–70% dimethyl copolymer cured for 12 h at 200 °C from United Chemical Technologies (Bristol, England) can be used. The obtained PDMS sheets were cut into slides of 1 × 10 × 100 mm³. The PDMS slides were coated with PEM without any further treatment to prevent cracks of oxidized PDMS, which occur upon elongation in the case of plasma-etched PDMS.¹⁵

Sample Preparation. The deposition method was LbL spraying deposition with a spraying time of 6 s for each solution, including rinsing with water.¹⁶ LbL dipping deposition¹ was also used to compare the film structure and dichroic ratio between both deposition methods as well as the validity of the approach presented here for both deposition methods (see the Supporting Information, Figure S2). Also, a preliminary polarized UV-absorption test with PEMs showed no orientation of the benzene ring for both deposition methods (data not shown). Despite the two different deposition methods relying on two different mechanisms (flow and diffusion controlled process),¹⁶ no differences of the molecular orientation of the molecules deposited by both methods were found. The deposition sequences were, in all cases, PDMS/PEI(PSS/PDMA)₁₆. The PEI deposition was performed from salt-free solution of PEI at pH 5 with a PEI concentration of 0.5 g/L. This assured formation of a single PEI layer on the support and good contact to the PDMS, as can be seen in refs 10 and 17.

In the case of PSS and PDMA deposition, two different salt concentrations (0 and 0.5 M NaCl, labeled as samples 1 and 2, respectively) were used to compare the influence of the ionic strength on the PEM elongation properties. Since only spectral intensities were compared, the fact that sample 2 is 3 times thicker than sample 1 and also contains much more PSS is not disturbing. The samples were stored until measurement in a desiccator at 100% relative humidity. This storage condition was chosen, because storage of the samples at an atmosphere

with a relative humidity lower than 15% causes formation of cracks in the PEM.¹⁷

ATR Measurement. To apply ATR experiments on a coated PDMS material, one needs to make sure that the PDMS is not changing its properties upon elongation, since, for comparison between the measurements, a substrate with a constant refractive index is needed.¹³ The change in the refractive index of the noncoated PDMS sheets upon elongation was, therefore, measured using ellipsometry. The PDMS sheets had a constant refractive index of 1.41 ± 0.01 (measured at a wavelength of 532 nm) upon elongation.¹⁸ This is expected for a nearly ideal elastic material like PDMS¹⁹ because the sheet shrinks on the side perpendicular to the elongation direction, thus keeping its density and refractive index constant. This result is important and shows that IR-ATR spectroscopy experiments with elongated PDMS are possible, because it assures a constant penetration depth of the evanescent IR wave and, therefore, makes the comparison of the IR spectra and the background subtraction possible.^{12,13}

The ATR setup was built by Fringeli (Optispec, Zuerich, Switzerland).¹³ The ATR plates applied for all experiments were 50 × 20 × 2 mm³ Ge trapezoids. An angle of incidence of 45° resulted in 25 internal reflections. The IR spectra were recorded with a Bruker Vertex 70 (Bruker, Billerica, MA) FTIR spectrometer equipped with a gold grid polarizer on a KRS-5 substrate and a sample baseline-sample reference (SBSR)-ATR mirror attachment. The SBSR technique allowed us to obtain a good baseline and the lowest possible fluctuations.¹³ Instead of a chopper, a computer-controlled lift was used to switch between sample and reference side.¹³ A computer-controlled rotatable polarizer was used to switch between vertical (V)- and parallel (P)-polarized light. In this setup, the parallel-polarized light is absorbed only by the *x* and *z* components of the oriented dipole moments of the sample, vertically polarized light only by the *y* components. Therefore, using an incidence angle of 45°, under isotropic conditions P- and V-polarized light is absorbed in the ratio of 2:1.¹³ The IR beam passed through 6 mm apertures and was detected by a mercury–cadmium–telluride detector. All spectra were scanned with 4 cm^{−1} resolution and a zero-filling factor of 2. The data recording and spectra processing was done with OPUS software version 5.053 (Bruker, Billerica, MA). To obtain a good signal-to-noise ratio, 100 spectra were summed up and averaged. The spectra processing was done by subtracting the PDMS marker bands (we chose the very specific Si–C=C bond vibration at 2100 cm^{−1}) from the PEM-PDMS measured spectra. The bands of the PEM spectra were fitted with OPUS software to obtain the peak areas, and the dichroic ratio (*R*) (the ratio between the absorbance peak areas of P- and V-polarized light) was calculated. The peak areas were obtained by fitting the spectra with Gaussian and/or Lorentzian peaks, but the detailed shape was not very important for the final conclusions. An example of successfully fitted spectra is presented in the Supporting Information, Figure S3.

The PDMS was fixed in the elongated and nonelongated states with a defined torque by squeezing it between an aluminum-covered OPTISPEC PEEK cell (liquid measurement cell) and the Ge ATR crystal by tightening the screws of the cell with a torque screwdriver. Two PDMS samples were measured at the same time by fixing one PDMS or PDMS-PEM sample on each half side of the crystal. Images of the sample and the PEEK cell are shown in the Supporting Information,

Figure S4, and the measurement setup is shown in the Supporting Information, Figure S5.

In the elongated/released state, the elongated/released spectra were subtracted from the nonelongated or weaker elongated sample before. Any later spectra that are named 5 or 15% in ATR are difference spectra compared to nonelongated or 5% elongated state (except when stated otherwise). This way one is able to observe the changes in spectra upon each elongation/release step. To compare the intensity of the peaks at different elongations, we assumed a constant refractive index of the PEM, which was proven by ellipsometry measurements.¹⁸ The PEM spectra were extracted from PEM-PDMS combination spectra by subtracting the PDMS spectra via OPUS software, as can be seen in the Supporting Information, Figure S6.

Film Elongation. The slides were first measured in the nonelongated state, then carefully elongated by $5 \pm 0.5\%$ (the elongation was observed with a ruler, therefore 10% relative error at 5% elongation) and fixed with sticky tape. The slides were then elongated by $15 \pm 0.5\%$ and afterward fully released. The spectra of bare IR-ATR crystals were measured after each experiment to check for remaining material from the PEM film and PDMS. During measurements, the relative humidity was $16 \pm 1\%$ by adjusting the air flow and the drying material in the measurement chamber. The humidity was observed constantly with a Rotronic Hygropalm 1 (Bassersdorf, Switzerland) and, in addition, by measuring the water content of the air before and after the measurements with the IR spectrometer.

RESULTS AND DISCUSSION

The quantitative measurements of pure PDMS showed upon elongations up to 5%, a significant decrease in density of the PDMS. At further elongations up to 15% and release, only a slight decrease in the absorption bands of the PDMS is found. We explain this finding with a peculiar Poisson ratio of PDMS rubber, which shrinks on the sides during uniaxial elongation. Therefore, the density of the material changes only slightly and the total absorption signal, which is proportional to the density, is (after some rearrangement of some regions close to the surface with a different density than the bulk)^{15,20,21} staying nearly constant. The measurements do not show an increasing order (change in dichroic ratio) of the molecules in the PDMS substrate upon elongation, data shown in Figure 1 and in the

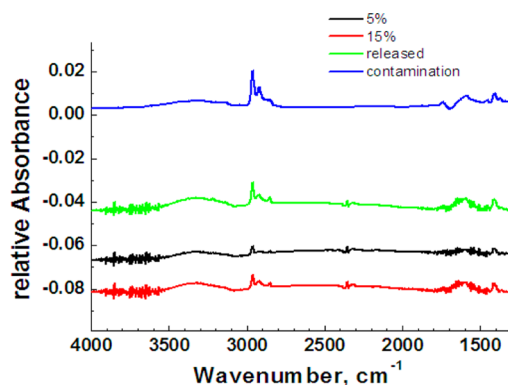


Figure 1. Change in absorbance spectra of P-polarized light relative to pristine sample upon different stages of elongation of pure PDMS. % = elongation of PDMS in percent; contamination refers to material on the ATR crystal after removal of the PDMS. See also the Supporting Information, Figure S7.

Supporting Information, Figure S7. The finding of no increasing order upon elongation can be explained with the fact that ATR is only able to detect the molecules very close to the surface of the PDMS. Here, the molecules experience a variety of different surface forces and shear forces, such as elongation in the stretching direction and compression and deformation from the side perpendicular to the elongation direction.^{10,15} Another reason is that the molecules might flip due to these forces only from vertical (x) to horizontal direction (z) or vice versa. Such changes would appear, however, in the two components in parallel (P)-polarized light and cannot be detected with the utilized setup. This decrease in surface density of elongated PDMS should be taken into account for elongated PDMS, especially in cases where the PDMS is coated, since it is not ideally elastic in this region. This finding is especially important since most current publications reporting surface effects consider PDMS ideally elastic.¹⁹ We would also like to point out that the used method to subtract the PDMS marker bands is a valid approach for the background subtraction, since the PDMS itself shows no sign of orientation change. A density decrease of 5–8% only in the area close to the interface has no big influence on the overall penetration depth of the evanescent wave, ensuring a constant measurement signal of the PEM. This approach is also supported by ellipsometry measurements using 532 nm, assuming homogeneous bulk PDMS during simulation, showing a nearly constant refractive index of the PDMS upon elongation.¹⁸

Abraded Material. After finishing the elongation and release measurements, a small amount of abraded PDMS on the ATR crystal was found, which was not oriented and, therefore, did not influence the measurement; see Figure 1. Measurements of the remains of the PEM on the ATR crystal showed that approximately $1/3$ of sample 1 and ca. $1/8$ of sample 2 were stuck as abrasion on the ATR crystal (values from sulfate absorption bands). This means that, approximately, the first 10 nm of both types of PEM was abraded; see the Supporting Information, Figure S8.

At this point, it is worth mentioning that the investigated type of PEM film breaks between 3 and 4% elongation (determined at 20% relative humidity; images not shown), which is in line with the literature, reporting a breakage of 5% at 30% relative humidity.¹⁷ An investigation of elongations above the point of breakage is of interest, since other groups reported elongations far above these elongation values.^{3,6}

Spectral Features of the Single PE the PEM Comprises. Absorption spectra of the single components, PEI, PSS, and PDMA, were obtained by adsorbing each component one after another onto the ATR crystal and subtracting the spectra of the precursor component. The corresponding spectra can be observed in the Supporting Information, Figure S9a,b. The strong overshoot of the PEI is due to absorption of water to the polyelectrolyte. The PEI causes absorption bands at 1429 cm^{-1} that correspond to the CH groups, whereas the absorptions at 1540 , 1642 , and 3410 cm^{-1} are caused by the NH groups. The absorption peaks at 1655 , 1562 , and 1475 cm^{-1} correspond to the PDMA. The peaks at 1650 , 1600 , and 1453 cm^{-1} belong to the aromatic group of the PSS, and its sulfate groups cause the absorption at 1410 cm^{-1} . The peak at 3442 cm^{-1} in the PSS spectra corresponds to water that is additionally adsorbed into the membrane. In the PDMA spectra, the peak at 3479 cm^{-1} corresponds to additional water that is absorbed into the PEM. Interestingly, the vibrational freedom of the water seems to be

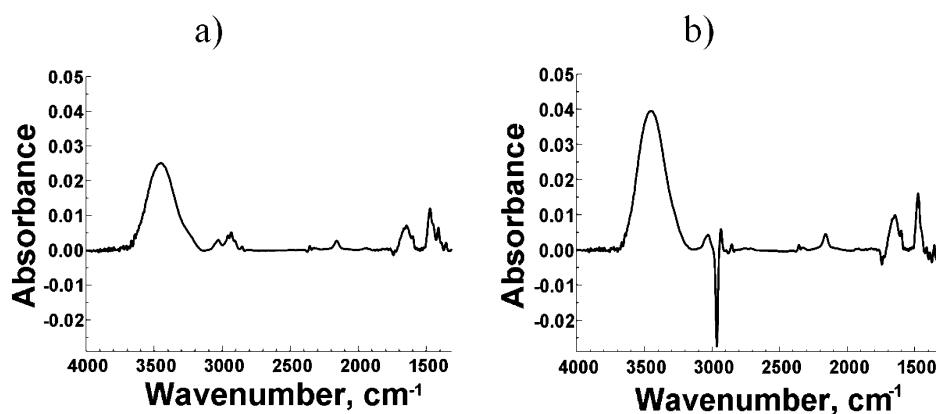


Figure 2. Absorbance spectra of PDMS-supported PEM in the nonelongated state of (a) PEM prepared without NaCl (sample 1) and (b) PEM prepared with NaCl (sample 2). The spectra of the pure PDMS were subtracted by using the PDMS specific vibration at 2100 cm^{-1} . Spectra shown were obtained by the use of P-polarized light.

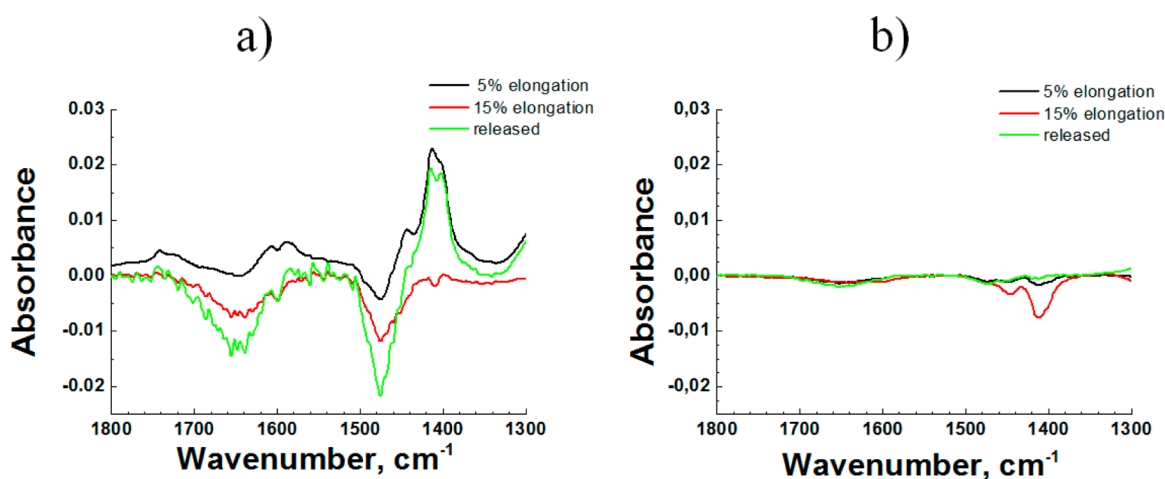


Figure 3. Absorbance spectra of PDMS-supported PEM in the nonelongated state of (a) PEM prepared with NaCl (sample 2) and (b) PEM prepared without NaCl (sample 1). The spectra of the pure PDMS were subtracted by using the PDMS specific vibration at 2100 cm^{-1} . Spectra shown were obtained by use of P-polarized light.

hindered, along with the PDDA deposition. This can be clearly seen by the overcompensation of large parts of the spectra, despite the adsorption of additional water; see the Supporting Information, Figure S9a. The absorption at 2925 cm^{-1} appearing in all spectra is due to the absorption of the carbohydrate backbone groups.

Spectral features of the PEM of both sample types on PDMS were exhibiting differences between the two sample types. Figure 2a,b presents the corrected spectra for samples 1 and 2, respectively. The spectra presented in Figure 2 show a strong IR absorption at 3450 cm^{-1} in the cases of both film types. This absorption is caused by incorporated water and also due to NH bonds of the PEI anchoring layer within the PEM. The PSS in the PEM samples causes aromatic vibrations at 1650 , 1600 , and 1475 cm^{-1} , and its sulfate groups cause the absorption at 1410 cm^{-1} .

Because of the preparation conditions causing slightly different orientations of the organic backbone of the PDMS substrate and the PEM, the CH bond vibrations at 2900 cm^{-1} are overcompensated and show as a result a negative absorption in the case of sample 2. The cause of these different orientations of the CH groups of the PDMS is the charge anisotropy within PEM prepared at high ionic strength.^{10,22,23} In return, it should be possible to influence the PEM internal

polarity anisotropy by a substrate exhibiting an anisotropic polarity. Certainly more work is needed to fully understand this effect. Despite its interesting properties and possibilities, this effect makes a quantitative study of the PEM backbone difficult and only allows a qualitative interpretation of the relative change of the PEM CH bond orientation (see Figure 2).

Upon elongation and release of sample 1, a reversible decrease in the observed CH groups (signal at $3000\text{--}2900\text{ cm}^{-1}$) was detected, whereas in the case of sample 2, the signal is irreversibly changed. The full individual spectra of PEM on PDMS are presented as the Supporting Information, Figures S10 and S11, respectively. The intensity of the ammonium, aromatic, and sulfate groups were for both types of PEM decreasing upon elongation; see Figure 3. This decrease in intensity upon elongation is caused by transportation of PEM out of the irradiated area. Upon release, the intensity is restored in the case of sample 1 (Figure 3b), but in the case of sample 2 (Figure 3a), the effect is irreversible.

The effect of a preparation-dependent reversibility of the absorption bands of the aromatic groups can be explained with the mechanical behavior of the PEM system. The PEM that was prepared without NaCl (sample 1) is “harder” (higher Young’s modulus) than that prepared with NaCl (sample 2).⁸ The cause for the influence of the ionic strength (NaCl content) of the

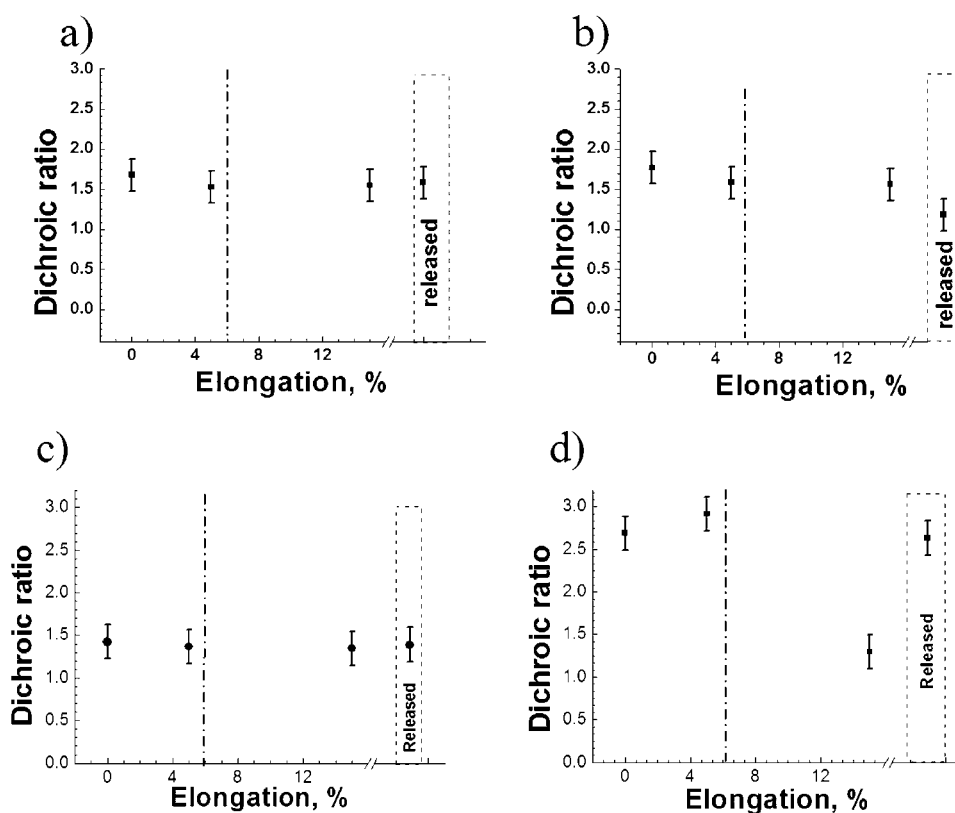


Figure 4. Dichroic ratios of PSS sulfonate groups (measured at 1410 cm^{-1} and shown on the right side (b, d)) and benzene groups (measured at 1647 cm^{-1} and shown on the left side (a, c)); sample 1 is (a) + (d) and sample 2 (b) + (c).

preparation solution on the mechanical properties of the resulting PEM is the charge shielding effect of the NaCl, which is shielding the ionic interactions and leads, therefore, to a relative increase of dispersive interactions as well as to a higher layer thickness.^{2,8} Therefore, the hard PEM of sample 1 breaks upon elongation and nearly no plastic deformation of the PEM occurred.

The PEM in the case of sample 2 is much softer²⁴ and can, therefore, plastically adapt its shape upon elongation. Since the PEM is harder than the PDMS, the PDMS is adapting to the elongated shape of the PEM, and therefore, it forms wrinkles upon release.³ These wrinkles prevent a uniform attachment of the PEM to the ATR crystal and cause, therefore, a bigger average distance of the PEM to the crystal. Since the evanescent wave decays exponentially with distance,¹³ a lower absorption signal is detected. At the same time, the dichroic ratio of the PDMS backbone is also reversed, which is a sign that the PDMS below the PEM is in a strongly elongated state. These qualitative results agree with the literature, assuming the mentioned effect based on mechanical measurements and utilizing it for calculation of the mechanical properties of the PEM films.³

Sample 2 shows additionally a decrease of the intensity of the water peak upon elongation. This effect is caused by the low humidity in the ATR setup and the fact that the PEM is becoming less dense upon elongation.^{18,21} The cause for the decrease in density of sample 2 upon elongation is the change in its internal hydrophilic nature alongside with a drastic change in its humidity-dependent swelling behavior; see ref 18.

Change in Dichroic Ratio of PSS Groups upon Elongation. To investigate the change of orientation in the PEM, the dichroic ratio was calculated. The dichroic ratio

depends on the orientation of the active molecular groups.^{13,25} Fraser's approach was applied for the calculations.²⁵ According to this, the dependence between the dichroic ratio measured in the applied geometry and the orientation of a molecule is (eqs 1 and 2)²⁵

$$R_{(\alpha)} = \frac{I_V}{I_P} = 2 \times \cot^2 \alpha \quad (1)$$

$$\alpha = \arctan\left(\sqrt{\frac{2}{R}}\right) \quad (2)$$

where R is the dichroic ratio and α is the position of the transition dipole moment relative to the coordinate system in which the dichroic ratio is measured, and I_V and I_P are the absorption intensities of the vertical (V)- and parallel (P)-polarized light.²⁵ An angle α of 54° corresponds, therefore, to an isotropic distribution of the transition dipole moments.²⁵ Since α is not a linear function and the relation of R to α is hard to imagine, the correlation is presented in the Supporting Information, Figure S12.

By calculating the dichroic ratio and α from the measured data, it is possible to track the rotation changes of molecular groups upon elongation. The benzene groups within the PEM of samples 1 and 2 show no sign of orientation change upon elongation, in contrast to the sulfate groups (see Figure 4a–d). This contradictory observation can be explained by the C–C single bond of benzene to the polymer backbone, as well as the C–S single bond of the benzene to the sulfate group. These single bonds allow rotational motion of the molecule. The benzene group appears, therefore, in P- and V-polarized light and, as a result, stay in the isotropic condition.

In contrast to the benzene groups, the sulfate groups that are covalently attached to the benzene groups are very sensitive to the elongation. This is because the sulfate group is bound by ionic interactions to the amino groups of the counter-polyelectrolyte.²² Therefore, the changes of the sulfate group correlate with the changes of the corresponding styrenesulphonate segments of the PSS.

In the case of sample 1, no change in orientation upon elongation was observed. This is caused by the strong ionic binding within sample 1, where the ionic binding between the PE is so strong that molecular reorientation is not possible. It seems that ripping of the PEM of sample 1 at high elongations (15%) leads to scattering artifacts. Otherwise, the sudden decay and restoration of the dichroic ratio of the sulfate peak cannot be explained (see Figure 4d). This artifact is caused by emerging cracks within the PEM, which are on the scale of several micrometers and are, therefore, interfering with the measurement light. Upon release of elongation, the distance between these cracks coalesces (relative to the measurement wavelength) and the artifact vanishes. Microscopic images showing the mentioned cracks upon elongation in the PEM can be observed in the Supporting Information, Figure S13.

In the case of sample 2, an irreversible decrease of the dichroic ratio upon elongation was detected, see Figure 4b). This effect is probably caused by ionic binding of sulfate groups to other binding sites upon elongation. The sulfate groups in sample 2 have a dichroic ratio of 1.8 ± 0.2 before elongating the sample, which corresponds according to Fraser's approach²³ to an angle α of $56.3^\circ \pm 2.1^\circ$, which is close to 54° , the angle of isotropic conditions. Upon elongation, the sample is becoming more and more anisotropic, and the dichroic ratio changes at 5% elongation to 1.6 ± 0.2 , which corresponds to an angle of $57.8^\circ \pm 2.0^\circ$, and does not change anymore during further elongation. Upon release, the dichroic ratio decreases to 1.2 ± 0.2 , which corresponds to an angle of $61.5^\circ \pm 1.6^\circ$. This change in dichroic ratio upon release is probably caused by an elongation of the PEM on top of the wrinkles, or by a restructuring of the PE during the wrinkling process. This finding is especially interesting, since this behavior should affect the properties of PEM-PDMS applications, such as gratings, based on the wrinkling effect. The probability that a scattering effect due to the surface structure leads to an artificially lower dichroic ratio can be excluded, since the wavelength of the wrinkling pattern (wavelength ~ 500 nm) is small compared to the wavelength of the used IR light (wavelength ~ 6500 nm).³

The results are able to support previous measurements performed on pyrene-labeled PSS containing PEM,¹⁰ where also an orientation change of the PE into the direction of elongation was detected. Interestingly, the orientation change of the sulfate group in the case of sample 2 is stronger than that of pyrene in ref 10. On the contrary, an orientation change in the sulfate groups in the case of sample 1 was not found, whereas an orientation change in ref 10 was observed. Both differences are attributed to the pyrene-induced lower charge density of the PSS, in the case of ref 10. The lowered charge density in the case of ref 10 caused a film that is softer than that of sample 1 investigated in this study. In the case of the difference of sample 2 to ref 10, it is expected that the lower charge density of the PE in ref 10 causes electrostatic blobs²⁶ that hinder reorientation. The result that a pyrene-labeling degree of 3% is already affecting mechanical and orientation properties of PE in PEM films is especially interesting since

other groups used this labeling degree assuming it would not affect the charge density of the polymer.²⁷

Influence of Elongation on PDDA and PEI. In the experiments, the amino group of the PEI was hidden below the water peak, and due to the low amount of PEI used in this study, other peaks were not sufficiently separated to draw a clear conclusion. The absorption peaks of the ammonium group of the PDDA at 1655 and 1475 cm^{-1} were partially convoluted with other peaks. The only peak that was measurable without bias from the PSS was the peak at 1562 cm^{-1} of the PDDA, which had, however, a contribution of 6.25% from the PEI, as can be seen in the Supporting Information, Figure S9. Upon elongation, this peak showed no change upon elongation, as can be seen in the Supporting Information, Figures S10 and S11. On the contrary, the peak at 1475 cm^{-1} showed a strong change in the absorption behavior. For this reason, the dichroic ratio for this peak was investigated. As can be seen in the Supporting Information, Figure S14, no orientation change of the PDDA for both sample types could be measured. This result is explained by the structure of the nitrogen of the PDDA or PEI. The structure of quarternary ammonium salts is the SP^3 structure.²⁸ The utilized setup is unable to detect the absorption of the quarternary ammonium group dependent from its molecular or polymer segment orientation. The change in the absorption peak was probably caused from density changes upon elongation.

Since the PEM film is, in the case of sample 1, not showing any shape deformation and just breaks, it is assumed that no molecular rearrangement for neither PSS nor the corresponding polycations PDDA and PEI is occurring. In the case of sample 2, the PEM film shows, upon elongation, a rather intact structure¹⁸ and no signs of charge separation were found. Therefore, it is assumed that the PDDA and PEI follow the orientation of the PSS. The permanent change of the CH groups upon elongation and release of sample 2, as can be observed in the Supporting Information, Figure S11, supports this theory as well. If the PDDA and PEI would not change their orientation in the same direction as the PSS, there would either be no, only be a very weak, or a contradictory change of the CH group direction detected. The remaining question that cannot be answered by this study is to which degree the PDDA and PEI follow the PSS orientation change.

CONCLUSION

The molecular orientation of PE in PEM experiencing uniaxial elongation can be studied quantitatively utilizing IR-ATR by simply pressing a coated flexible substrate with a constant pressure onto the ATR crystal. Utilizing this method, it was possible to observe a decrease in the PDMS density close to the surface upon elongation, despite current theory considering this material ideally elastic. It was also possible to measure the formation of wrinkles due to an increased average distance of the PEM to the ATR crystal (in the case of PEM prepared at high ionic strength). It is also shown that the PEM prepared at high ionic strength influences the orientation of the PDMS backbone close to the surface in the nonelongated state and changes this orientation also irreversibly upon elongation and release. This effect was not observed in the case of PEM prepared at low ionic strength. This unexpected effect of the influence of the ionic strength on the PDMS substrate is attributed to anisotropy of the polarity within the PEM.

In the case of a PEM prepared at high ionic strength, the sulfate groups change their orientation in the PEM, whereas the

benzene groups show no sign of orientation change, due to their rotational symmetry and our measurement setup. The sulfate groups increase their alignment, when the PEM is released, indicating an elongation of the PEM on top of the wrinkles. Within the PEM prepared at low ionic strength, the polyelectrolytes are not able to change their orientation upon elongation and the PEM preferably breaks.

■ ASSOCIATED CONTENT

● Supporting Information

The Supporting Information contains (1) a drawing of the PSS and the PDDA used, (2) comparison of anisotropy from dipping and spraying technique, (3) curve fitting in OPUS software, (4) PEEK cell used for fixation of the sample, (5) a figure showing the used ATR setup schematically, (6) spectra of pure PDMS, coated PDMS, and subtracted spectra, (7) examples of pristine and differential spectra of PDMS, (8) remaining contamination of PEM on ATR crystal after measurement, (9) spectra of single polyelectrolyte components (PEI, PSS, and PDDA) in the PEM, (10) elongated differential spectra of both polarizations of sample 1, (11) elongated differential spectra of both polarizations of sample 2, (12) dependence of dichroic ratio on angle α , (13) cracks emerging after 5% elongation, and (14) dichroic ratio versus elongation for the PDDA. This material is available free of charge via the Internet at <http://pubs.acs.org>.

■ AUTHOR INFORMATION

Corresponding Author

*E-mail: johannes.frueh@hit.edu.cn (J.F.), qianghe@hit.edu.cn (Q.H.).

Author Contributions

The manuscript was written through contributions of all authors. All authors have given approval to the final version of the manuscript.

Notes

The authors declare no competing financial interest.

■ ACKNOWLEDGMENTS

We would like to thank Zhipeng Wang and Ralf Köhler for helpful discussions. We would like to thank DFG (project number KR3432/1-1), Max Plank Society, EU-FP7 Marie Curie Staff Exchange Scheme (No. 269159), and Harbin Institute of Technology for the financial support.

■ REFERENCES

- (1) Decher, G.; Hong, J. D.; Schmitt, J. Build Up of Ultrathin Multilayer Films by a Self-Assembly Process: III. Consecutively Alternating Adsorption of Anionic and Cationic Polyelectrolytes on Charged Surfaces. *Thin Solid Films* **1992**, *210–211*, 831–835.
- (2) Klitzing, R. v. Internal Structure of Polyelectrolyte Multilayer Assemblies. *Phys. Chem. Chem. Phys.* **2006**, *8*, 5012–5033.
- (3) Nolte, A. J.; Rubner, M. F.; Cohen, R. E. Determining the Young's Modulus of Polyelectrolyte Multilayer Films via Stress-Induced Mechanical Buckling Instabilities. *Macromolecules* **2005**, *38*, 5367–5370.
- (4) Richter, R. P.; Berat, R.; Brisson, A. R. Formation of Solid-Supported Lipid Bilayers: An Integrated View. *Langmuir* **2006**, *22*, 3497–3505.
- (5) Ross, E. E.; Spratt, T.; Liu, S.; Rozanski, L. J.; O'Brien, D. F.; Saavedra, S. S. Planar Supported Lipid Bilayer Polymers Formed by Vesicle Fusion. 2. Adsorption of Bovine Serum Albumin. *Langmuir* **2003**, *19*, 1766–1774.
- (6) Hemmerle, J.; Roucoules, V.; Fleith, G.; Nardin, M.; Ball, V.; Lavalle, P.; Marie, P.; Voegel, J. C.; Schaaf, P. Mechanically Responsive Films of Variable Hydrophobicity Made of Polyelectrolyte Multilayers. *Langmuir* **2005**, *21*, 10328–10331.
- (7) Mertz, D.; Vogt, C.; Hemmerlé, J.; Mutterer, J.; Ball, V.; Voegel, J.-C.; Schaaf, P.; Lavalle, P. Mechanotransductive Surfaces for Reversible Biocatalysis Activation. *Nat. Mater.* **2009**, *8*, 731–5.
- (8) Pavoov, P. V.; Bellare, A.; Strom, A.; Yang, D.; Cohen, R. E. Mechanical Characterization of Polyelectrolyte Multilayers Using Quasi-Static Nanoindentation. *Macromolecules* **2004**, *37*, 4865–4871.
- (9) Mertz, D.; Hemmerlé, J.; Boulmedais, F.; Voegel, J.-C.; Lavalle, P.; Schaaf, P. Polyelectrolyte Multilayer Films under Mechanical Stretch. *Soft Matter* **2007**, *3*, 1413–1420.
- (10) Frueh, J.; Reiter, G.; Möhwald, H.; He, Q.; Krastev, R. Orientation Change of Polyelectrolytes in Linearly Elongated Polyelectrolyte Multilayer Measured by Polarized UV Spectroscopy. *Colloids Surf., A* **2012**, *415*, 366–373.
- (11) Tedeshi, C.; Li, L.; Möhwald, H.; Spitz, C.; von Seggern, D.; Menzel, R.; Kirchstein, S. Engineering of Layer-by-Layer Coated Capsules with the Prospect of Materials for Effect and Direct Electron Transfer. *J. Am. Chem. Soc.* **2004**, *126*, 3218–3227.
- (12) Matijević, J.; Hassler, N.; Reiter, G.; Fringeli, U. P. In situ ATR FTIR Monitoring of the Formation of Functionalized Mono- and Multilayers on Germanium Substrate: From 7-Octenyltrichlorosilane to 7-Carboxylsilane. *Langmuir* **2008**, *24*, 2588–96.
- (13) Fringeli, U. P.; Goette, J.; Reiter, G.; Siam, M.; Baurecht, D. Structural Investigations of Oriented Membrane Assemblies by FTIR-ATR Spectroscopy. *AIP Conf. Proc.* **1998**, No. 430, 729–747.
- (14) Flournoy, P. A. Attenuated Total Reflection from Oriented Polypropylene Films. *Spectrochim. Acta* **1964**, *22*, 15–20.
- (15) Frueh, J.; Nakashima, N.; He, Q.; Moehwald, H. Effect of Linear Elongation on Carbon Nanotube and Polyelectrolyte Structures in PDMS-Supported Nanocomposite LbL Films. *J. Phys. Chem. B* **2012**, *116*, 12257–12262.
- (16) Schlenoff, J. B.; Dubas, S. T.; Farhat, T. Sprayed Polyelectrolyte Multilayers. *Langmuir* **2000**, *16*, 9968–9969.
- (17) Frueh, J.; Koehler, R.; Moehwald, H.; Krastev, R. Changes of the Molecular Structure in Polyelectrolyte Multilayers under Stress. *Langmuir* **2010**, *26*, 15516–15522.
- (18) Frueh, J.; Reiter, G.; Moehwald, H.; He, Q.; Krastev, R. Novel Controllable Auxetic Effect of Linearly Elongated Supported Polyelectrolyte Multilayer with Amorphous Structure. *Phys. Chem. Chem. Phys.* **2013**, *15*, 483–488.
- (19) Huang, X.-J.; Kim, D.-H.; Im, M.; Lee, J.-H.; Yoon, J.-B.; Choi, Y.-K. "Lock-and-Key" Geometry Effect of Patterned Surfaces: Wettability and Switching of Adhesive Force. *Small* **2009**, *5*, 90–94.
- (20) Takayanagi, M.; Imada, K.; Kajiyama, T. Mechanical Properties and Fine Structure of Drawn Polymers. *J. Polym. Sci. C* **1967**, *15*, 263–281.
- (21) Frueh, J. Structural Change of Polyelectrolyte Multilayers under Mechanical Stress. Dissertation, Max-Planck-Institute of Colloids and Interfaces, Potsdam, Germany, 2011; p 194.
- (22) Schönhoff, M. Layered Polyelectrolyte Complexes: Physics of Formation and Molecular Properties. *Condens. Matter* **2003**, *15*, 1781–1808.
- (23) DeWitt, D. Studying and Controlling Chromophore Orientation in Polyelectrolyte Layer-by-Layer Thin Films. Ph.D. Thesis, Massachusetts Institute of Technology, Cambridge, MA, 2002; pp 1–162.
- (24) Park, J.; Hammond, P. T. Polyelectrolyte Multilayer Formation on Neutral Hydrophobic Surfaces. *Macromolecules* **2005**, *38*, 10542–10550.
- (25) Fraser, R. D. B. The Interpretation of Infrared Dichroism in Fibrous Protein Structures. *J. Chem. Phys.* **1953**, *21*, 1511–1515.
- (26) Borue, V. Y.; Erukhimovich, I. Y. A Statistical Theory of Weakly Charged Polyelectrolytes: Fluctuations, Equation of State, and Microphase Separation. *Macromolecules* **1988**, *21*, 3240–3249.

- (27) Li, L.; Möhwald, H. Photoinduced Vectorial Charge Transfer across Walls of Hollow Microcapsules. *Angew. Chem.* **2004**, *116*, 364–367.
- (28) Babiacyk, W. I.; Bonella, S.; Guidoni, L.; Ciccotti, G. Hydration Structure of the Quaternary Ammonium Cations. *J. Phys. Chem. B* **2010**, *114*, 15018–28.